Electronic Supplementary Material (ESI) for Materials Horizons.

n-Type Boron *β*-Diketone-Containing Conjugated Polymer for High-Performance Room Temperature Ammonia Sensor

Weichen Song‡[a], Jiankun Sun‡[a], Qian Wang‡[a], Han Wu[a], Kunpeng Zheng[a], Binbin Wang[a], Zhong Wang[b], and Xiaojing Long[a]*

[a] State Key Laboratory of Bio-fibers and Eco-textiles, Collaborative Innovation Center of Shandong Marine Biobased Fibers and Ecological Textiles, Institute of Marine Biobased Materials, College of Materials Science and Engineering, Qingdao University, Qingdao 266071, P. R. China. longxj@qdu.edu.cn.

[b] Qingdao Institute of Bioenergy and Bioprocess Technology, Chinese Academy of Sciences, Qingdao 266071, P. R. China

Content

1. Experimental details

Statistical Analysis

1. Pre-processing of data: PXRD, TG, UV-vis, XPS, in-situ FT-IR, I-V, and ammonia sensing data were converted into TXT format by the corresponding instruments, and plotted by Origin software without normalization and evaluation of outliers. The data of SEM, TEM, and DFT calculations were in the form of pictures or numbers, which were directly drawn by PowerPoint software without conversion, normalization, and evaluation of outliers.

2. Software used for statistical analysis: The related software was Origin, PowerPoint, and GraphPad Prism.

2. Thermogravimetric analysis

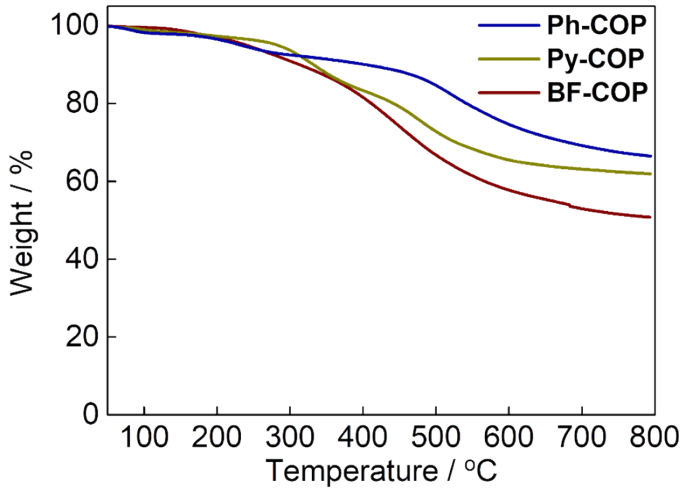

Figure S1. TGA curves of **Ph-COP**, **Py-COP**, and **BF-COP**.

3. Morphology and specific surface area

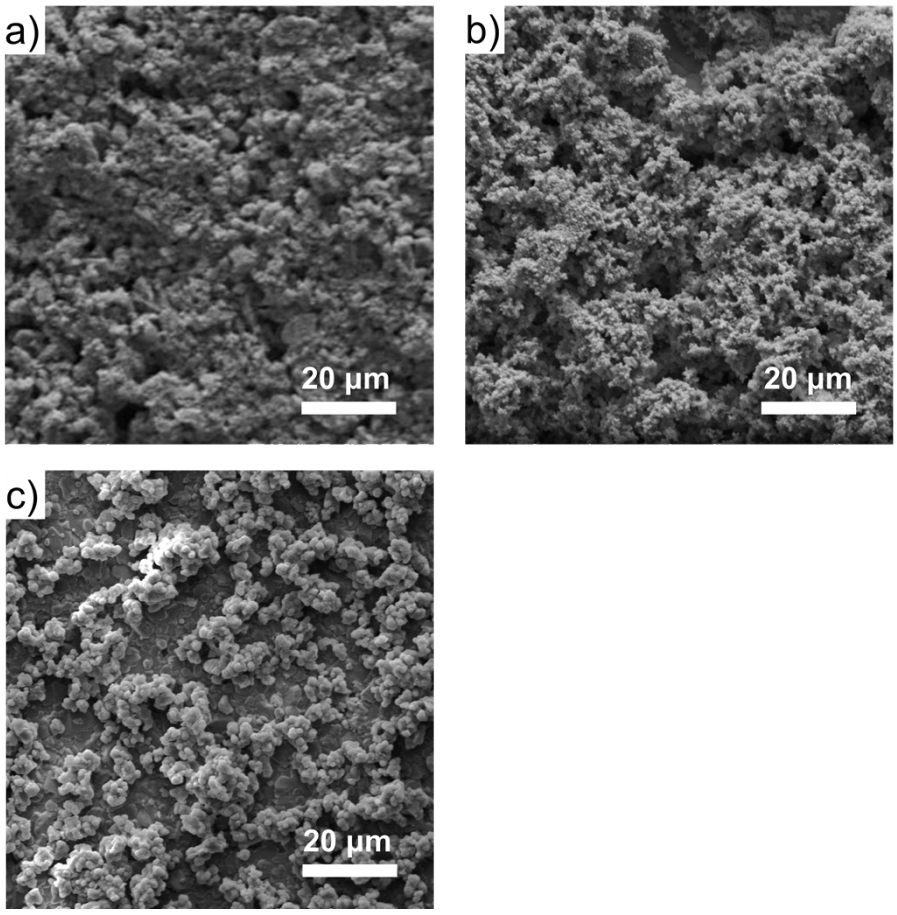

Figure S2. SEM of a) **Ph-COP**, b) **Py-COP**, and c) **BF-COP** on the interdigital electrodes.

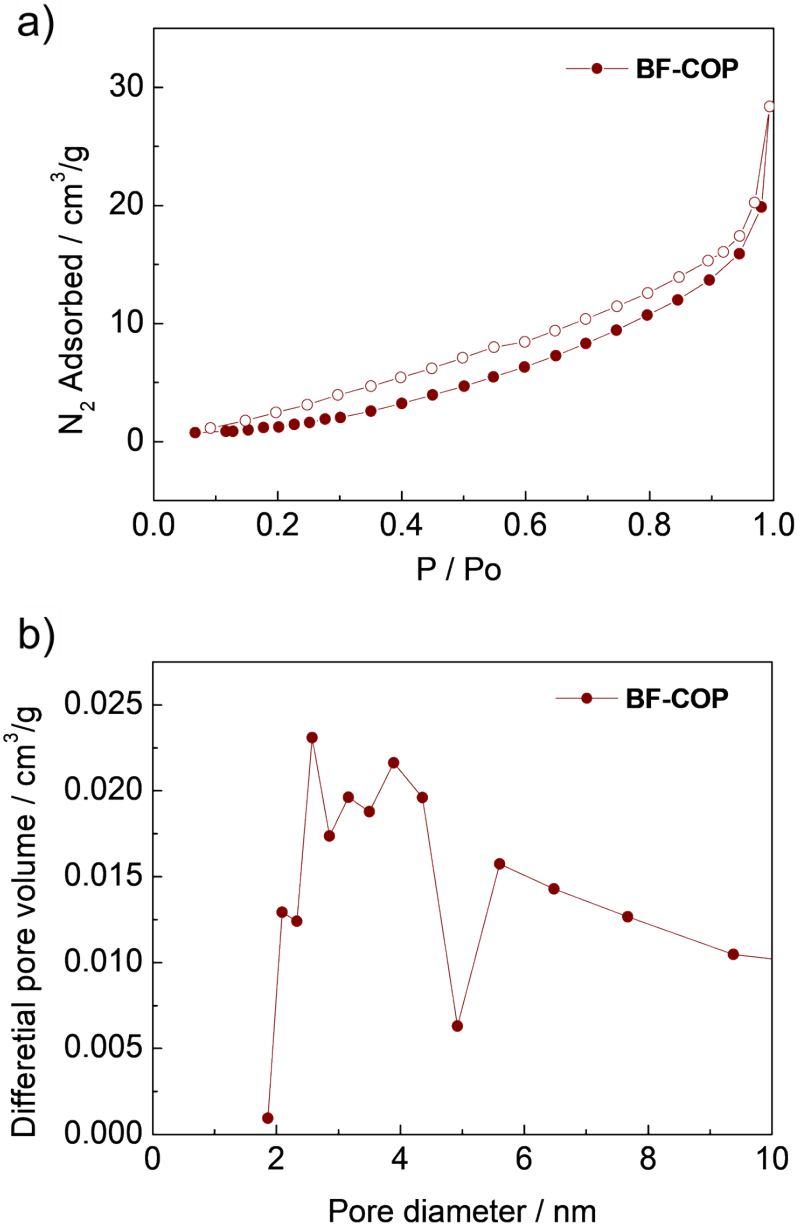

Figure S3. a) N_2 adsorption isotherm (filled symbols) and desorption isotherm (open symbols) at 77 K and b) pore size distribution of **BF-COP**.

4. DFT calculations

The structural optimizations and DFT calculations of the model compounds **Ph-COP Py-COP**, and **BF-COP** were performed using the Gaussian 09 program at the B3LYP/6-31G(d,p) level of theory.[1]

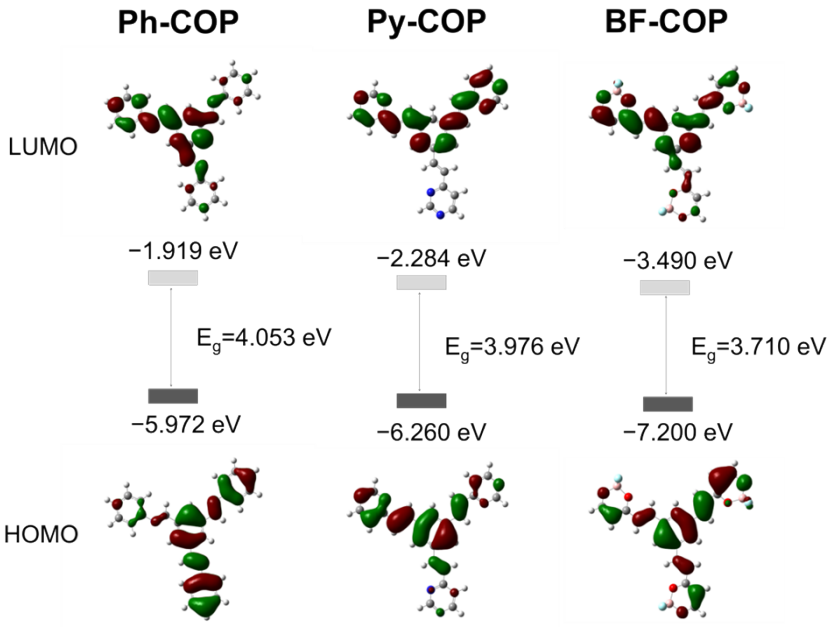

Figure S4. The optimized structures and Kohn-Sham LUMOs and HOMOs of the model compounds of **Ph-COP**, **Py-COP**, and **BF-COP**.

5. Fluorescence properties

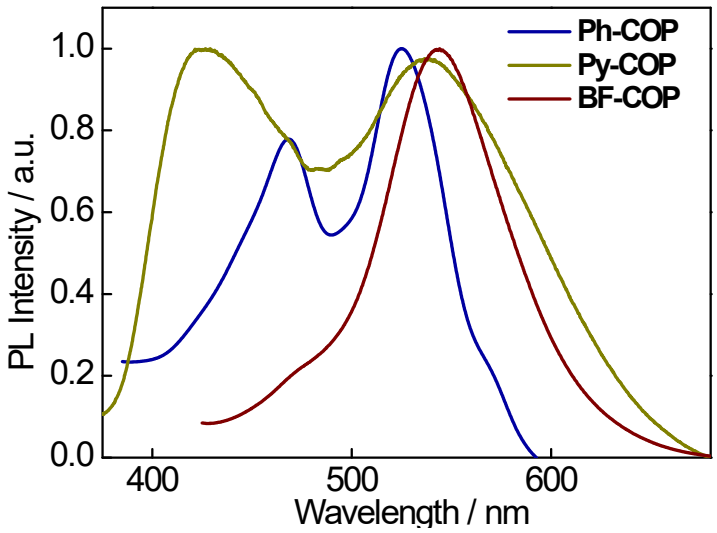

Figure S5. Room-temperature photoluminescence (PL) emission spectra of **Ph-COP**, **Py-COP**, and **BF-COP** powders.

6. Gas sensing performance

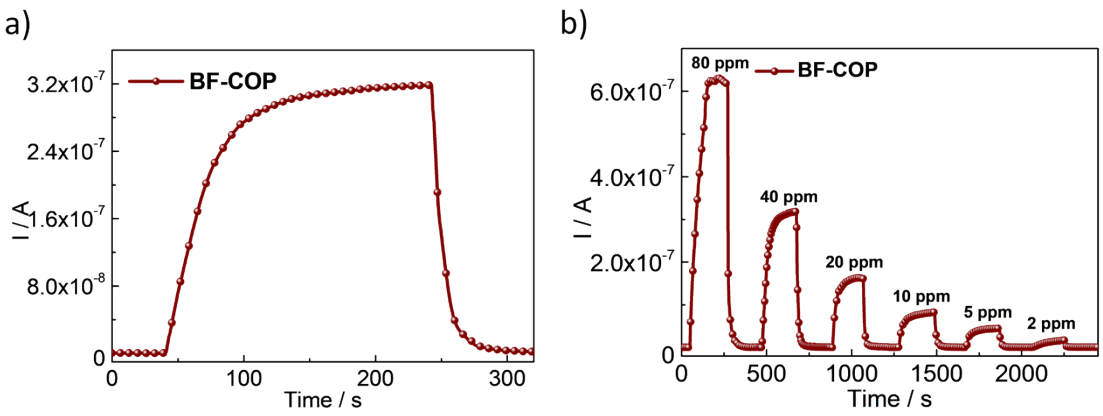

Figure S6. The real-time current response/recovery curve of the **BF-COP** sensor.

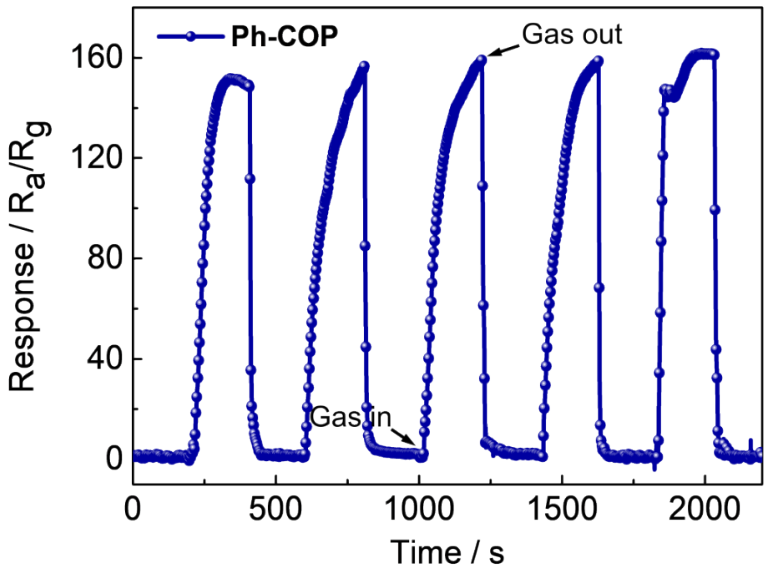

Figure S7. The response-recovery curve of the **Ph-COP** sensor to 40 ppm NH_3 at room temperature.

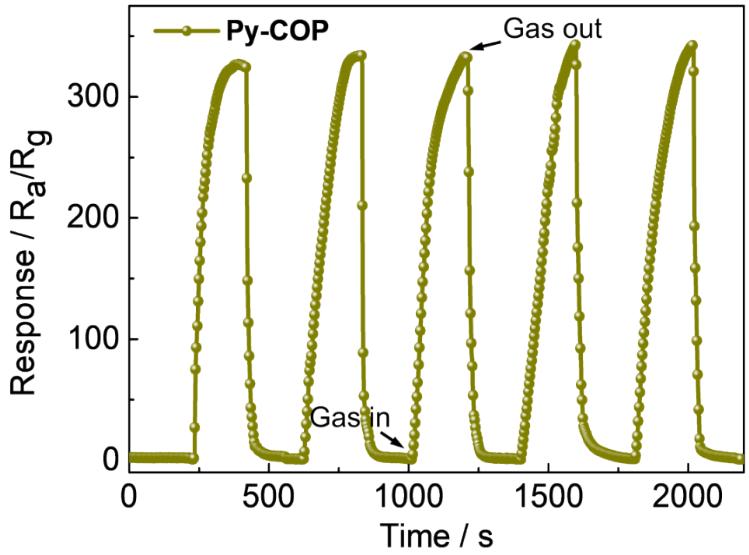

Figure S8. The response-recovery curve of the **Py-COP** sensor to 40 ppm NH_3 at room temperature.

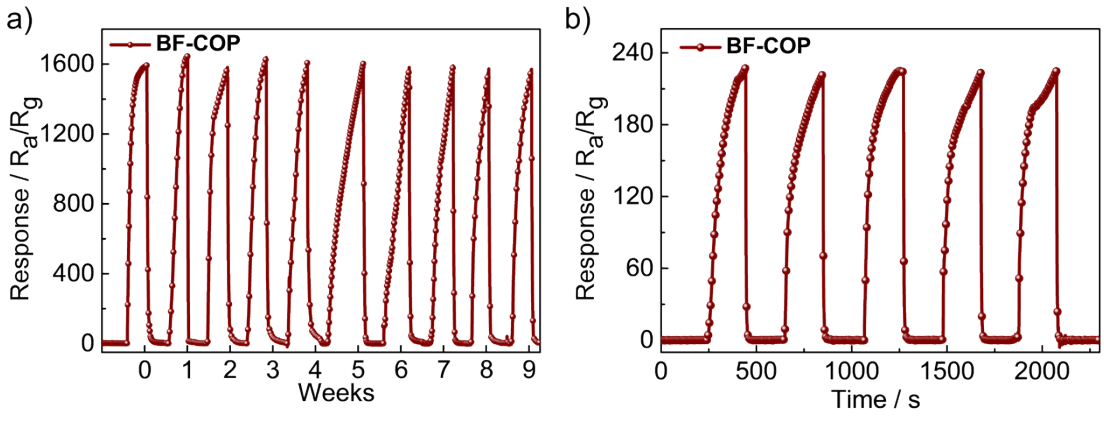

Figure S9. The real-time response-recovery curve of the **BF-COP** sensor to a) 40 ppm within two months and b) 5 ppm NH_3 at room temperature.

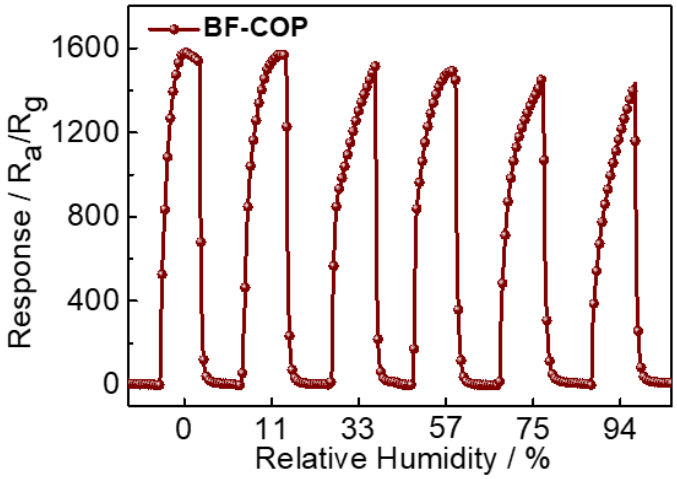

Figure S10. The real-time response-recovery curve of the **BF-COP** sensor under different relative humidity.

7. Stability and anti-interference tests

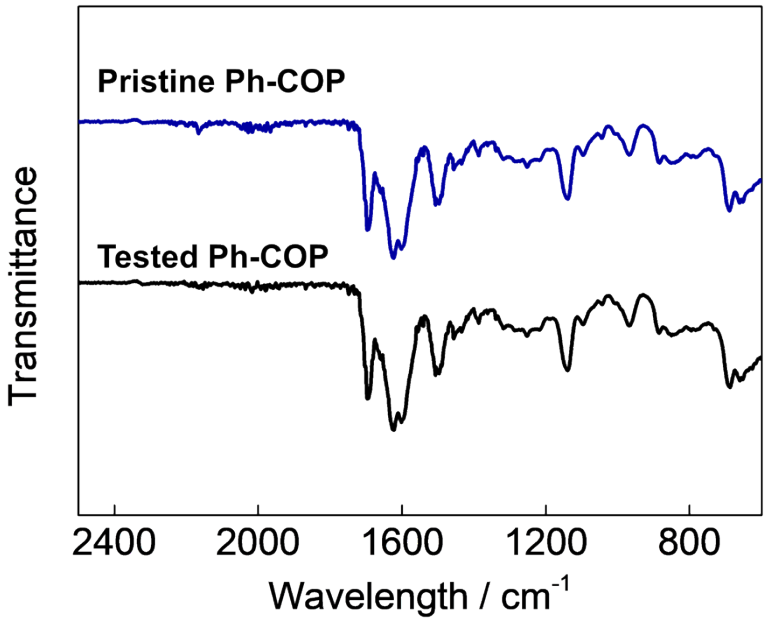

Figure S11. The infrared spectrum of **Ph-COP** before and after sensing tests.

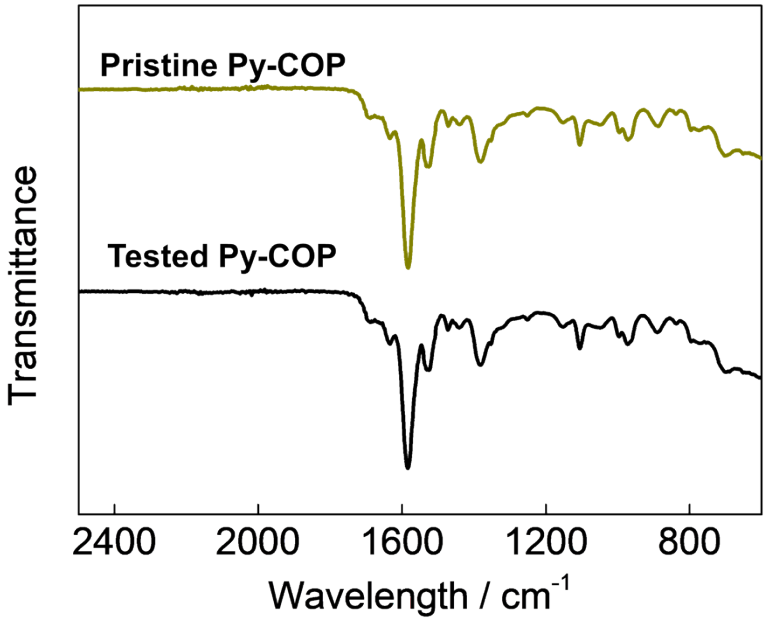

Figure S12. The infrared spectrum of **Py-COP** before and after sensing tests.

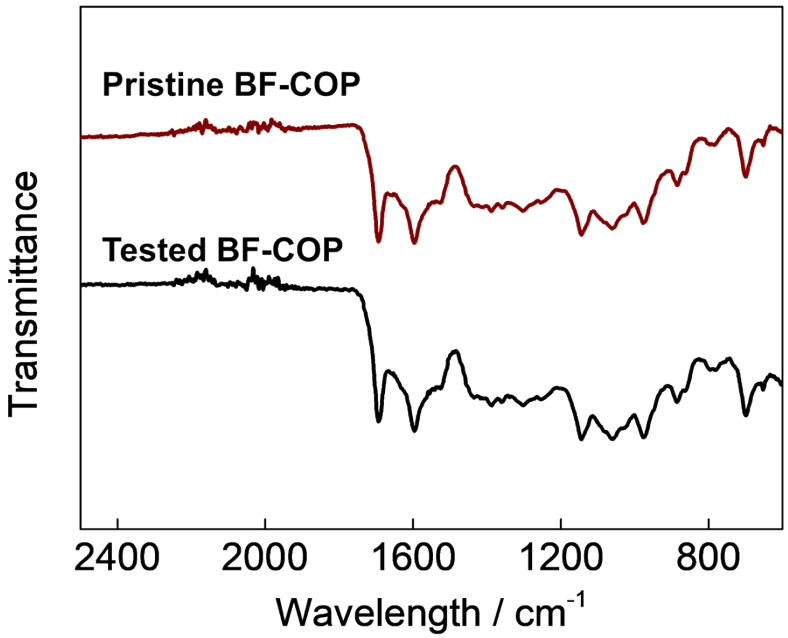

Figure S13. The infrared spectrum of **BF-COP** before and after sensing tests.

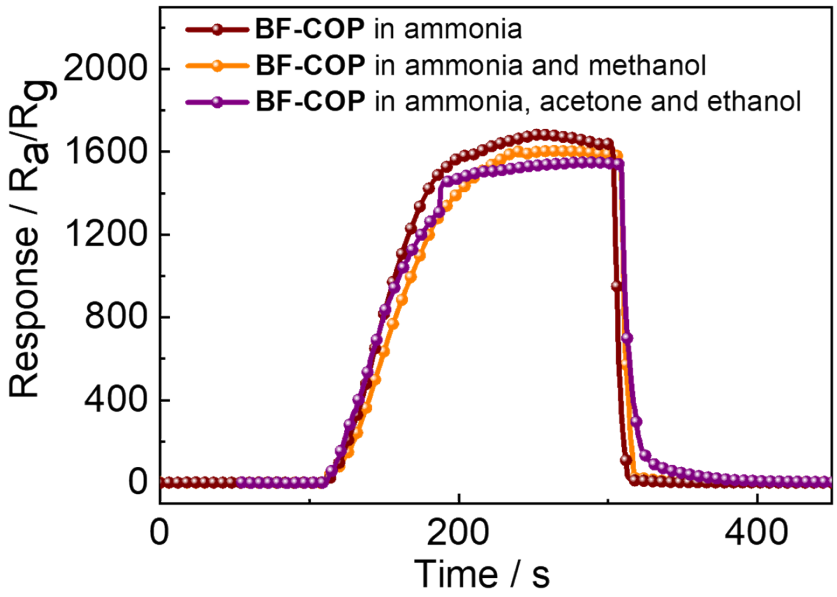

Figure S14. The anti-interference performance of the **BF-COP** sensor in the mixture of ammonia, methanol, acetone and ethanol.

8. X-ray photoelectron spectroscopy

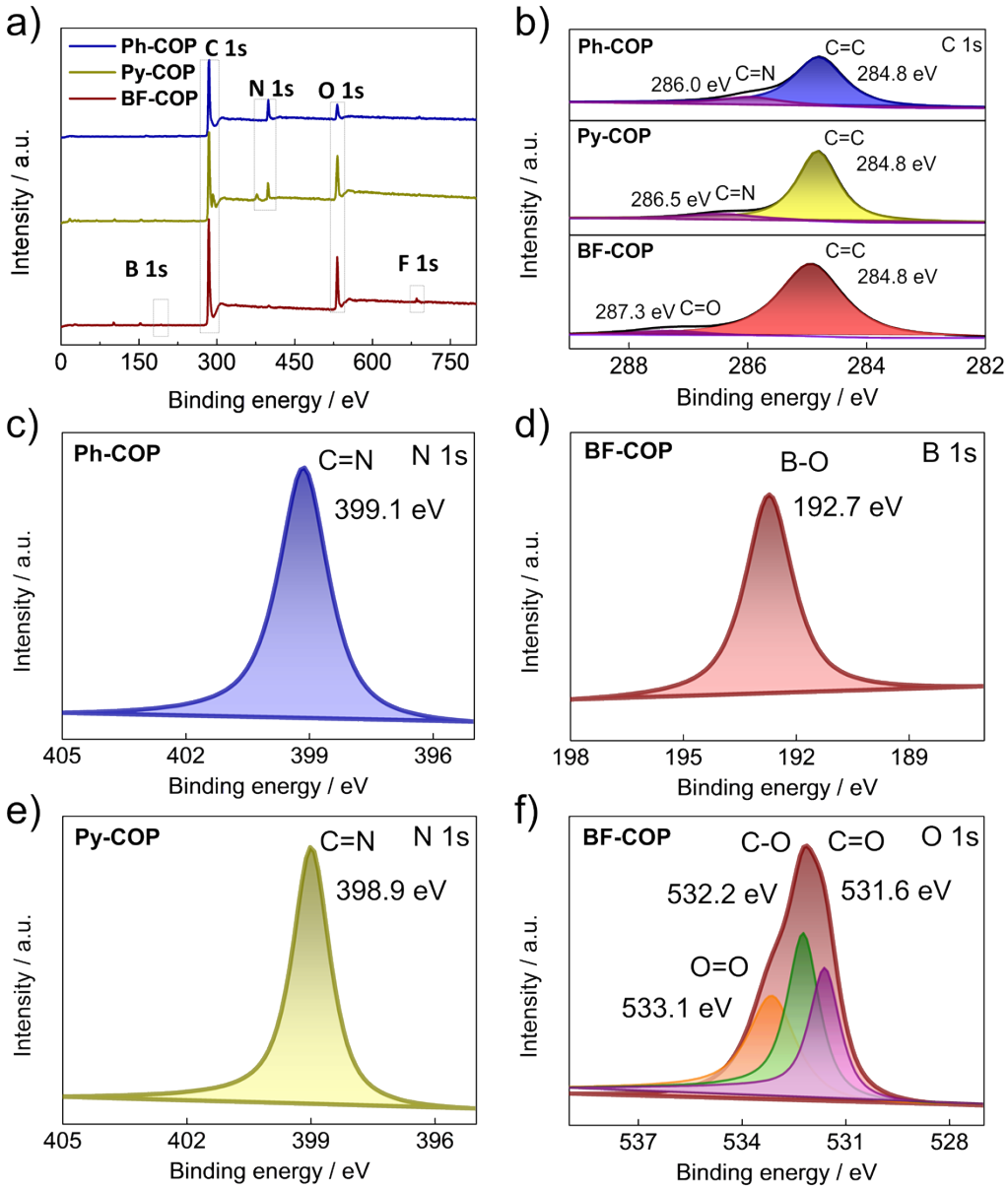

Figure S15. High-resolution XPS spectra of a) survey; b) C 1s of **Ph-COP**, **Py-COP**, and **BF-COP**; c) N 1s for **Ph-COP**; d) B 1s for **BF-COP**; e) N 1s for **Py-COP** and f) O 1s for **BF-COP**.

9. NMR spectra

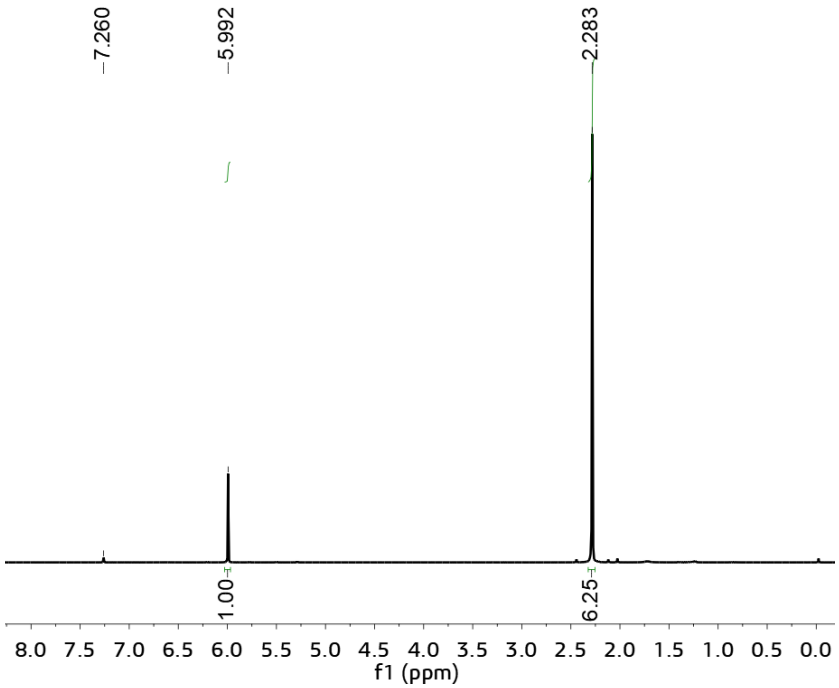

Figure S16. ^{1}H NMR spectrum of **BF** monomer.

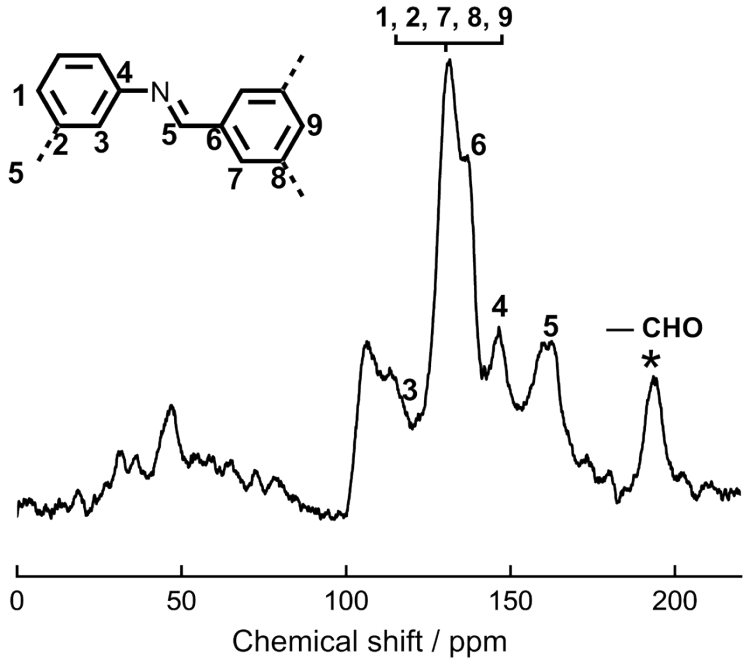

Figure S17. Solid-state ^{13}C NMR spectrum of **Ph-COP**.

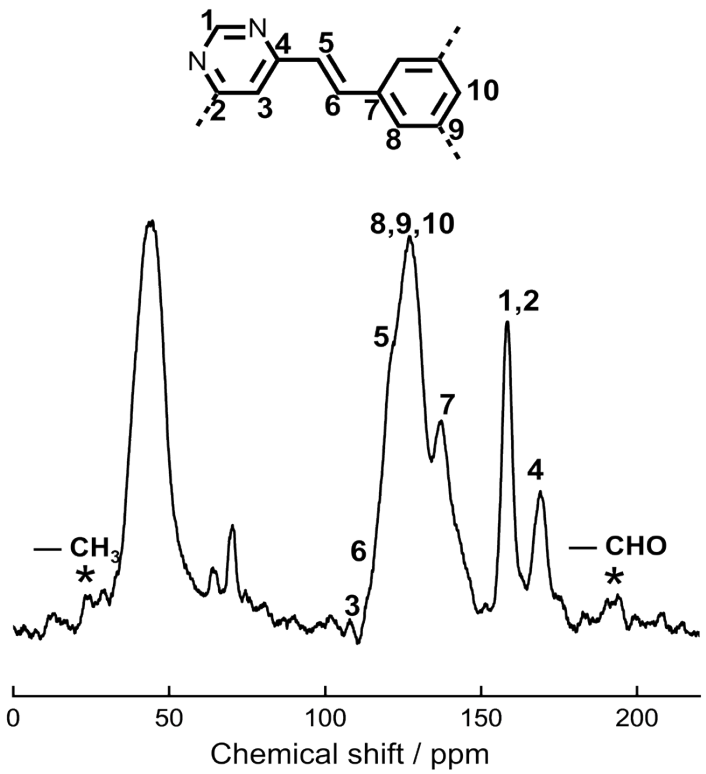

Figure S18. Solid-state ^{13}C NMR spectrum of **Py-COP**.

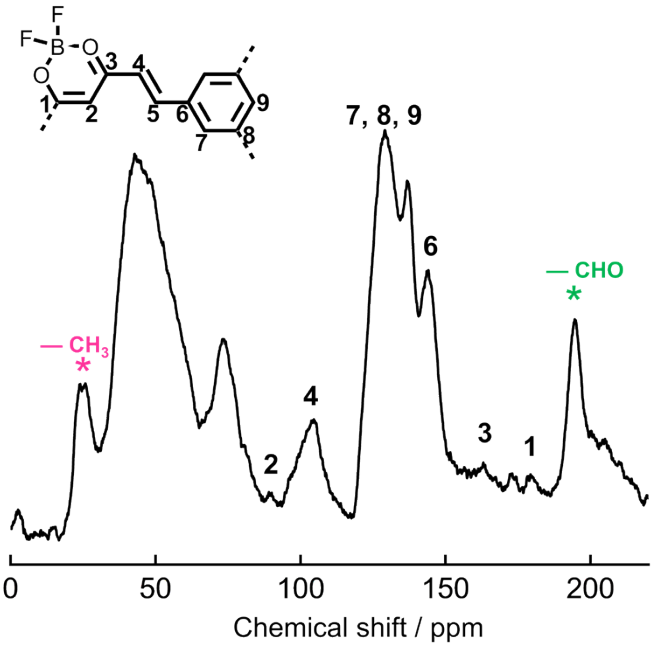

Figure S19. Solid-state ^{13}C NMR spectrum of **BF-COP**.

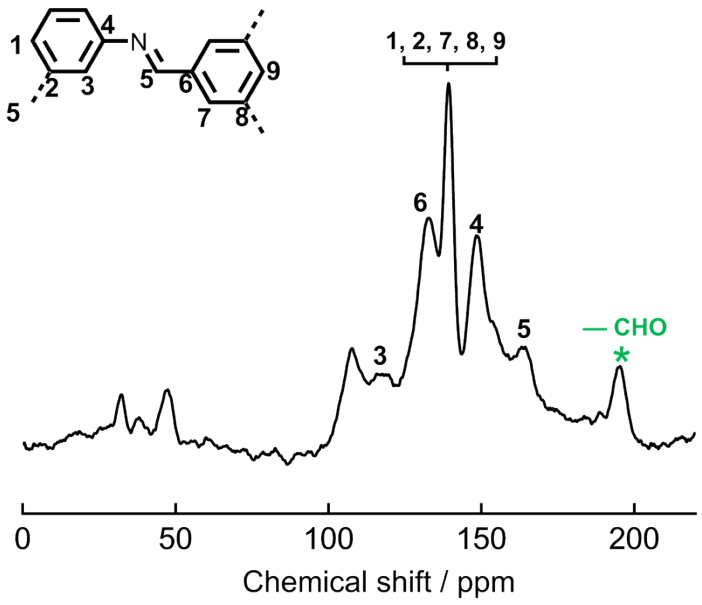

Figure S20. Solid-state ^{13}C NMR spectrum of **Ph-COP** after exposing to ammonia.

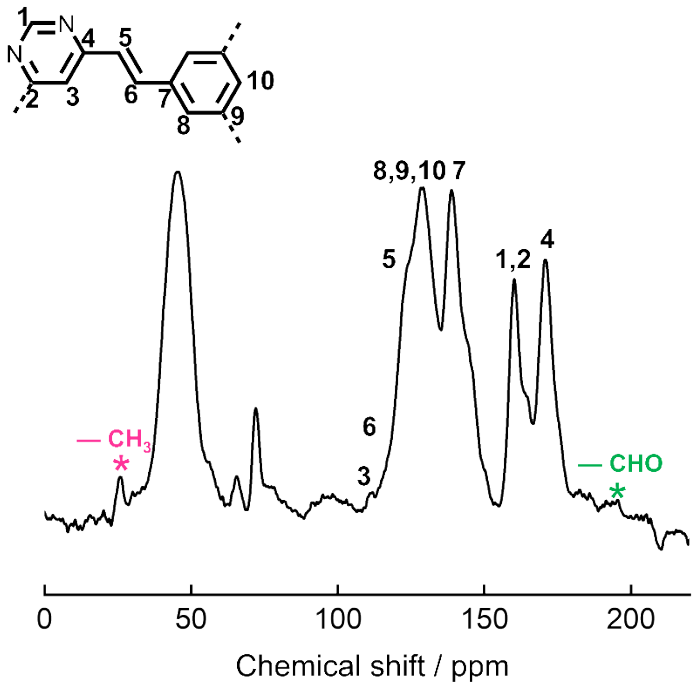

Figure S21. Solid-state ^{13}C NMR spectrum of **Py-COP** after exposing to ammonia.

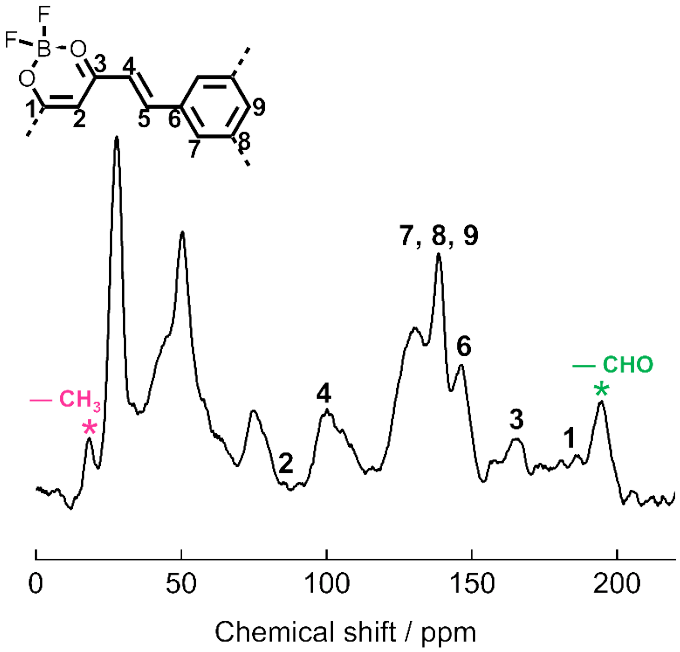

Figure S22. Solid-state ^{13}C NMR spectrum of **BF-COP** after exposing to ammonia.

10. Supplementary references

[1] Gaussian 09 (Revision A.02), M. J. Frisch, G. W. Trucks, H. B. Schlegel, G. E. Scuseria, M. A. Robb, J. R. Cheeseman, G. Scalmani, V. Barone, B. Mennucci, G. A. Petersson, H. Nakatsuji, M. Caricato, X. Li, H. P. Hratchian, A. F. Izmaylov, J. Bloino, G. Zheng, J. L. Sonnenberg, M. Hada, M. Ehara, K. Toyota, R. Fukuda, J. Hasegawa, M. Ishida, T. Nakajima, Y. Honda, O. Kitao, H. Nakai, T. Vreven, J. A. Montgomery, Jr., J. E. Peralta, F. Ogliaro, M. Bearpark, J. J. Heyd, E. Brothers, K. N. Kudin, V. N. Staroverov, R. Kobayashi, J. Normand, K. Raghavachari, A. Rendell, J. C. Burant, S. S. Iyengar, J. Tomasi, M. Cossi, N. Rega, J. M. Millam, M. Klene, J. E. Knox, J. B. Cross, V. Bakken, C. Adamo, J. Jaramillo, R. Gomperts, R. E. Stratmann, O. Yazyev, A. J. Austin, R. Cammi, C. Pomelli, J. W. Ochterski, R. L. Martin, K. Morokuma, V. G. Zakrzewski, G. A. Voth, P. Salvador, J. J. Dannenberg, S. Dapprich, A. D. Daniels, Ö. Farkas, J. B. Foresman, J. V. Ortiz, J. Cioslowski, D. J. Fox, Gaussian, Inc., Wallingford CT, 2009.